Heterobinuclear Methyl Complexes of Rhodium/Iridium: Reactivity with Nucleophiles and Subsequent Ligand Rearrangements

Okemona Oke, Robert McDonald,† and Martin Cowie*

Department of Chemistry, University of Alberta, Edmonton, Alberta, Canada T6G 2G2

Received November 24, 1998

Reaction of $[RhIr(CH_3)(CO)_3(dppm)_2][CF_3SO_3]$ (**1**) (dppm = $Ph_2PCH_2PPh_2$) with several phosphines and phosphites yields the carbonyl-substitution products $[RhIr(CH_3)(PR_3)(CO)_2(dppm)_2][CF_3SO_3]$ (**4**), in which the added phosphine and the methyl ligands are coordinated to Ir. At −80 °C an intermediate in this reaction, $[RhIr(CH_3)(PR_3)(CO)_3(dppm)_2][CF_3SO_3]$ (**3**), is observed in which the monodentate PR_3 group is bound to Rh. Similar reactions with the dicarbonyl compound $[RhIr(CH_3)(CO)_2(dppm)_2][CF_3SO_3]$ (**2**) suggests that attack occurs directly at Ir in this case. The structure of **2** is subtly different in solution and in the solid state, having the carbonyls both terminally bound (one to each metal) in solution, but having one bridging in the solid. Addition of cyanide and hydride ligands to **2** yields the neutral products $[RhIr(CH_3)X(CO)_2(dppm)_2]$ (X = CN, H), in which both anionic ligands (X and CH_3) are bound to Ir. The hydrido species is unstable, eliminating methane at ambient temperature. Addition of iodide ion to **2** yields the related neutral species, which has the methyl group on Rh and the iodide ligand on Ir. The X-ray structures of compounds **2** and **4a** (PR_3 = PMe_3) are reported. Compound **2** has a terminal carbonyl on Rh, essentially opposite the Rh−Ir bond, the methyl group in a similar position on Ir, and a semibridging carbonyl, which is more tightly bound to Ir. The geometry of **4a** has a square-planar Rh center in which Ir occupies one of the coordination sites opposite a carbonyl, and an octahedral Ir center in which the PMe_3 group is opposite the Ir−Rh bond, and the methyl group is opposite the second carbonyl. The crowding at Ir upon addition of the PMe_3 group shows up in a number of distortions within the molecule.

Downloaded by CARLI CONSORTIUM on June 30, 2009
Published on April 8, 1999 on http://pubs.acs.org | doi: 10.1021/om980947y

Introduction

The reaction of the diiridium, dicarbonyl methyl complex $[Ir_2(CH_3)(CO)_2(dppm)_2][CF_3SO_3]$ with a variety of small molecules results in the unusually facile C−H bond cleavage of the methyl group by the adjacent metal to give the methylene-bridged products $[Ir_2H(CO)_2L(\mu\text{-}CH_2)(dppm)_2][SO_3CF_3]$ (L = CO, SO_2, CNR, PR_3).[1] Related studies with the mixed Rh/Ir tricarbonyl complex $[RhIr(CH_3)(CO)_3(dppm)_2][CF_3SO_3]$ (**1**) have yielded very different results.[2] Whereas reaction of **1** with CO gave rise to a number of uncharacterized products, reaction with SO_2 gave an acyl product in which the methyl group has migrated to a carbonyl and the added SO_2 molecule bridges the metals, and reaction with ^{t}BuNC gave an iminoacyl-bridged species resulting from loss of a carbonyl and migratory insertion of the methyl and isocyanide groups. The products of these reactions were often the result of carbonyl substitution by the added ligand, to give complexes having stoichiometries analogous to the methylene-bridged diiridium products, but no example of C−H bond cleavage was observed for the Rh/Ir compounds. In attempts to learn more about the factors influencing the reactivity of methyl groups in the presence of adjacent metal centers, we have extended our studies on the reactivity of the mixed Rh/Ir methyl complex **1**, to include the dicarbonyl complex $[RhIr(CH_3)(CO)_2(dppm)_2][CF_3SO_3]$ (**2**). We were interested in determining the sites of ligand attack in these two species, the subsequent ligand rearrangements that occur, and the roles of the different metals in the chemistry.

Although methyl-bridged species were implicated throughout the studies of the diiridium complexes, they were only proposed as transient intermediates and were never observed. It was reasoned that the lower tendency of Rh to oxidatively add across a C−H bond[3] might allow the isolation (or at least observation) of such methyl-bridged species. We have therefore undertaken a study of the reactivity of complexes **1** and **2** with a number of phosphines and phosphites and with a few anionic nucleophiles in attempts to learn more about the binding and subsequent activation of methyl groups under a range of electronic and steric environments.

* Fax: (780)492-8231. E-mail: martin.cowie@ualberta.ca.
† Faculty Service Officer, Structure Determination Laboratory.

(1) (a) Antwi-Nsiah, F.; Cowie, M. *Organometallics* **1992**, *11*, 3157. (b) Torkelson, J. R.; Antwi-Nsiah, F. H.; McDonald, R.; Cowie, M.; Pruis, J. G.; Jalkanen, K. J.; DeKock, R. L. *J. Am. Chem. Soc.*, in press.

(2) (a) Antwi-Nsiah, F. H.; Oke, O.; Cowie, M. *Organometallics* **1996**, *15*, 506. (b) Antwi-Nsiah, F. H.; Oke, O.; Cowie, M. *Organometallics* **1996**, *15*, 1042.

(3) Collman, J. P.; Hegedus, L. S.; Norton, J. R.; Finke, R. G. *Principles and Applications of Organotransition Metal Chemistry*; University Science Books: Mill Valley, CA, 1987; p 239.

10.1021/om980947y CCC: $18.00 © 1999 American Chemical Society
Publication on Web 04/08/1999

Downloaded by CARLI CONSORTIUM on June 30, 2009
Published on April 8, 1999 on http://pubs.acs.org | doi: 10.1021/om980947y

Experimental Section

General Comments. All solvents were appropriately dried and distilled prior to use and were stored under dinitrogen. Deuterated solvents used for NMR experiments were degassed and stored under dinitrogen over molecular sieves. Reactions were carried out routinely at room temperature (unless otherwise stated) and under standard Schlenk conditions; compounds that were isolated as solids were purified by recrystallization. Hydrated rhodium trichloride was purchased from Engelhard Scientific, whereas all the phosphines and phosphites, silver trifluoromethanesulfonate (AgOTf), Super-Hydride (lithium triethylborohydride (1.0 M solution in THF)), tetrabutylammonium cyanide (96%), and trimethylamine *N*-oxide were obtained from Aldrich and were used as received. Potassium iodide was purchased from BDH Chemicals, while ^{13}CO was supplied by Isotec Inc. All gases were used as received. The compound $[RhIr(CH_3)(CO)_3(dppm)_2][CF_3SO_3]$[2b] (**1**) was prepared as previously reported, while the compounds $[RhIr(CH_3)(CO)_2(PR_3)(dppm)_2][CF_3SO_3]$ (**4a**, R = Me; **4b**, R = OPh)[4] were previously prepared but incompletely characterized.

All routine NMR experiments were conducted on a Bruker AM-400 spectrometer, whereas the $^{13}C\{^{31}P\}$ experiments were conducted on a Bruker AM-200 spectrometer operating at 50.32 MHz. $^1H-^{13}C$ HMQC experiments were carried out on a Varian Unity 500 MHz spectrometer. The solid-state $^{13}C-\{^1H\}$ NMR spectrum was recorded on a Bruker AMR-300 spectrometer (with MAS accessory) operating at 75.5 MHz. Infrared spectra were obtained on a Nicolet 7199 Fourier transform or a Perkin-Elmer 883 IR spectrometer, either as Nujol mulls on KBr plates or as solutions in KCl cells with 0.5 mm window path lengths. Elemental analyses were performed by the microanalytical service within our department. Spectroscopic data for all compounds are given in Table 1.

Preparation of Compounds. (a) $[RhIr(CH_3)(CO)_2(dppm)_2][CF_3SO_3]$ (2). Compound **1** (60 mg, 0.046 mmol) was dissolved in 20 mL of CH_2Cl_2 and was gently refluxed under a slow dinitrogen purge (ca. 0.2 mL s^{-1}) for 1 h, during which time the orange color of the solution deepened slightly. Removal of the solvent under vacuum and recrystallization from CH_2Cl_2/ether gave a bright orange solid (53 mg, 90% yield). Anal. Calcd for $IrRhSP_4F_3O_5C_{54}H_{47}$: C, 50.51; H, 3.66. Found: C, 50.23; H, 3.45.

(b) Low-Temperature Reaction of Compounds 1 and 2 with Phosphines and Phosphites. In an NMR tube, 30 mg (0.023 mmol) of compound **1** was dissolved in 0.6 mL of CD_2Cl_2 under N_2. The solution was then cooled to ca. −80 °C by immersion in a dry ice/acetone bath. PMe_3 (46 μL of 1 M THF solution) was added via a syringe, and the mixture was taken immediately for NMR analysis. The $^{31}P\{^1H\}$ and ^1H NMR data were collected at −60 °C, while $^{13}C\{^1H\}$ NMR analysis was carried out at −40 °C. The NMR spectra showed the presence of $[RhIr(CH_3)(CO)_3(PMe_3)(dppm)_2][CF_3SO_3]$ (**3a**). Upon gradually warming the sample to 0 °C, **3a** was replaced by $[RhIr(CH_3)(CO)_2(PMe_3)(dppm)_2][CF_3SO_3]$ (**4a**). A similar procedure was performed for $P(OPh)_3$, $PPh(OMe)_2$, and $PPhMe_2$ for which the species **3b**−**d**, respectively, were observed in solution. For the reaction of compound **2** and PMe_3, the procedure was as described above except that 1 equiv of PMe_3 was used for the reaction, and NMR data were collected at −100 °C. Only compound **4a** was observed in solution at this temperature.

(c) $[RhIr(CH_3)(CO)_2(PR_2R')(dppm)_2][CF_3SO_3]$ (R=R′ = Me (4a); R=R′ = OPh (4b); R = Me, R′ = Ph (4c); R = OMe, R′ = Ph (4d)). A solution of 1 equiv of neat PMe_3 (97%, 15.7 μL, 0.076 mmol) was syringed into a 100 mL flask containing 100 mg (0.076 mmol) of **1** dissolved in 10 mL of CH_2Cl_2, causing the dark orange solution to turn yellow immediately. The mixture was stirred for 2 h, after which the solvent was removed in vacuo. Recrystallization from CH_2Cl_2/ether yielded a yellow microcrystalline solid (65 mg, 68% yield). Anal. Calcd for **4a**, $IrRhSP_5F_3O_5C_{57}H_{56}$: C, 50.29; H, 4.11. Found: C, 50.34; H, 3.91. In the preparation of **4b**−**d**, the procedure is the same as described for **4a** except that the reactions were carried out using 1 equiv each of $P(OPh)_3$, $PPhMe_2$ and $PPh(OMe)_2$, respectively. Anal. Calcd for **4b**, $IrRhSP_5F_3O_8C_{72}H_{62}$: C, 54.24; H, 3.92. Found: C, 54.19; H, 3.96 (85 mg, 70% yield). Anal. Calcd for **4c**, $IrRhSP_5F_3O_5C_{62}H_{58}$: C, 52.31; H, 4.08. Found: C, 52.23; H, 3.70 (83 mg, 77% yield). Anal. Calcd for **4d**, $IrRhSP_5F_3O_7C_{62}H_{58}$: C, 51.16; H, 3.99. Found: C, 50.74; H, 4.13.

(d) $[RhIr(CH_3)(PR_2R')(\mu\text{-}CO)(dppm)_2][CF_3SO_3]$ (R = R′ = Me (5a), R = Me, R′ = Ph (5c)). Compound **4a** (50 mg, 0.037 mmol) and a large excess of Me_3NO (14 mg, 0.187 mmol) were charged into a 50 mL flask and dissolved in 10 mL of CH_2Cl_2, and the resulting mixture was stirred under a slow N_2 flow for 6 h, during which time the yellow color of the starting material turned deep orange. The solution was taken to dryness in vacuo and redissolved in ca. 1 mL of CH_2Cl_2. A dark brown-orange solid was precipitated upon addition of 5 mL of ether. The product was separated by filtration, washed twice with 5 mL of ether, and dried under N_2 flow and in vacuo overnight. The procedure for preparing **5c** was similar except that the reaction time was 2 h. Microanalyses for **5a** and **5c** consistently gave variable results due to difficulties in separating the excess Me_3NO used in these reactions.

(e) $[RhIr(CH_3)(CN)(CO)_2(dppm)_2]$ (6). A 30 mg (0.023 mmol) sample of compound **2** and 7 mg (0.026 mmol) of tetrabutylammonium cyanide were charged into an NMR tube and dissolved in 0.5 mL of THF-d_8, causing an immediate color change from orange to pale yellow. The sample was immediately taken for NMR analysis. Attempts to isolate the product resulted in formation of an intractable oil.

(f) Reaction of Compound 2 with Super-Hydride. A 30 mg (0.023 mmol) sample of **2** was dissloved in 0.5 mL of CD_2Cl_2 in an NMR tube at −80 °C. Approximately 1 equiv of Super-Hydride ($LiHBEt_3$), (23 μL of 1 M THF solution, 0.023 mmol) was syringed into the solution. NMR data were collected immediately. The compound $[RhIr(CH_3)(H)(CO)_2(dppm)_2][CF_3SO_3]$ (**7**) was shown to be the major ^{31}P-containing species at this temperature. The sample was then gradually warmed to room temperature over a 0.5 h period causing the appearance of $[RhIr(CO)_2(\mu\text{-}H)(\mu_2\text{-}\eta^3\text{-}(o\text{-}C_6H_4)P(Ph)CH_2PPh_2)(dppm)]$ (**8**), the tricarbonyl species $[RhIr(CO)_3(dppm)_2]$, and several unidentified decomposition products. Compound **8** was never successfully separated from the tricarbonyl and other species, so was only characterized by NMR spectroscopy.

(g) $[RhIr(CH_3)(I)(CO)_2(dppm)_2]$ (9). A 60 mg (0.046 mmol) sample of **2** was dissolved in 10 mL of acetone. Slightly more than 1 equiv of KI (8 mg, 0.048 mmol), dissolved in 5 mL of acetone, was added via an addition funnel to a stirring solution of **2** over a 0.5 h period, causing a slow color change from orange to yellow. The mixture was stirred for 1 h, and the solvent volume was then removed, to give an orange-yellow residue. The product was extracted with 3 mL of CH_2Cl_2, filtered through a frit, after which the solvent was removed in vacuo, and then redissolved in 1 mL of acetone. A yellow solid precipitated upon addition of 5 mL of pentane and which was washed once with 5 mL of pentane, dried under N_2 stream and then in vacuo. Microanalysis consistently gave variable results due to contamination with $[RhIr(I)_2(CO)_2(dppm)_2]$, which was identified in the sample and has been previously characterized.[5]

X-ray Data Collection for $[RhIr(CH_3)(CO)_2(dppm)_2][CF_3SO_3]$ (2). Orange crystals of 2 were obtained by slow diffusion of ether into a concentrated solution of the compound.

(4) Antwi-Nsiah, F. H. Ph.D. Thesis, University of Alberta, 1994; Chapter 2.

(5) Vaartstra, B. A.; Xiao, J.; Jenkins, J. A.; Verhagen, R.; Cowie, M. *Organometallics* **1991**, *10*, 2708.

Downloaded by CARLI CONSORTIUM on June 30, 2009
Published on April 8, 1999 on http://pubs.acs.org | doi: 10.1021/om980947y

Table 1. Spectroscopic Parameters for the Compounds[a]

compounds	IR,[b] cm^{-1}	NMR[d] δ (^{31}P{^{1}H})	δ (^{1}H)	δ (^{13}C{^{1}H})
[RhIr(CH$_3$)(CO)$_2$(dppm)$_2$][CF$_3$SO$_3$] (**2**)	1954(ss);[c] 1858(bs), 1997(ms)	22.2−22.8(second-order multiplet)	4.27(m,2H), 3.84(m,2H), 0.59(t,3H)[g]	184.9(dm,$^1J_{RhC}$=7Hz,1C), 175.4(dt,$^1J_{RhC}$=73Hz,1C)[f]
[RhIr(CH$_3$)(CO)$_3$(PMe$_3$)(dppm)$_2$][CF$_3$SO$_3$] (**3a**)		29.6(ddm,$^1J_{RhP}$=121Hz), −19.6(m), −35.4(dt,$^1J_{RhP}$=147Hz, $^2J_{PP}$=30Hz)[g]	4.75(m,2H), 2.74(m,2H), −0.14(t,3H), 0.60(d,$^2J_{PH}$=11Hz,9H)[g]	262.7(dm,$^1J_{RhC}$=25Hz,1C), 202.4(ddm,$^1J_{RhC}$=53Hz,1C), 185.1(ddt,$^2J_{CC}$=$^2J_{RhC}$=14Hz,1C)[f]
[RhIr(CH$_3$)(CO)$_3$(P(OPh)$_3$)(dppm)$_2$][CF$_3$SO$_3$] (**3b**)		126.3(dt,$^1J_{RhP}$=190Hz), 27.2(ddm, $^1J_{RhP}$=144Hz,$^2J_{PP}$=49Hz), −21(m)[g]	4.61(m,2H), 4.94(m,2H), 0.65(t,3H)[g]	232.8(bs,1C), 185.3(dm, $^1J_{RhC}$=31Hz,1C), 186(ddm, $^1J_{RhC}$=64Hz,1C)[f]
[RhIr(CH$_3$)(CO)$_3$(PPh(Me)$_2$)(dppm)$_2$][CF$_3$SO$_3$] (**3c**)		28.8(ddm,$^1J_{RhP}$=105Hz), −32.5 (dt, $^1J_{RhP}$=129Hz,$^2J_{PP}$=36Hz), −17.6(m)[g]	4.58(m,2H), 2.90(m,2H), 1.06(d,$^2J_{PH}$=7Hz,6H), −0.08(t,3H)[g]	260.2(dm,$^1J_{RhC}$=12Hz,1C), 201.1(ddm,$^1J_{RhC}$=65Hz,1C) 187.7(bs,1C)[f]
[RhIr(CH$_3$)(CO)$_3$(PPh(OMe)$_2$(dppm)$_2$][CF$_3$SO$_3$] (**3d**)		153.0(dt,$^1J_{RhP}$=157Hz,$^2J_{PP}$=54Hz), 27.4(ddm,$^1J_{RhP}$=134Hz), −17.0(m)[g]	4.94(m,2H), 4.62(m,2H), 3.92(d,$^2J_{PH}$=6Hz,6H), 0.41(t,3H)[g]	233.9(dm,$^1J_{RhC}$=10Hz,1C), 190.7(ddt,$^1J_{RhC}$=64Hz, $^2J_{PC}$ =15Hz,1C), 185.0 (m,1C)[f]
[RhIr(CH$_3$)(CO)$_2$(PMe$_3$)(dppm)$_2$][CF$_3$SO$_3$] (**4a**)[f]	2028(ms), 1956 (ss)	12.6(dm,$^1J_{RhP}$=131Hz), 6.4(dm,$^1J_{RhP}$=126Hz), −23.5(m), −32.7(m), −62.4(m)	5.55(m,1H), 5.08(m,1H), 4.82(m,1H), 4.77(m,1H), 0.33(dt,$^3J_{PH}$=8Hz, $^3J_{PH}$=14Hz,3H), 0.23(d,9H)	182.4(dm,$^1J_{RhC}$=68Hz,1C), 178.7(m,1C)
[RhIr(CH$_3$)(CO)$_2$(P(OPh)$_3$)(dppm)$_2$][CF$_3$SO$_3$] (**4b**)[f]	1980(ms), 1955(ss)	58.2(m), 15.7(dm,$^1J_{RhP}$=129Hz), 6.9(dm,$^1J_{RhP}$=123Hz), −22.9(m), −23.9(m)	5.55(m,1H), 5.06(m,1H), 4.65(m,1H), 4.60(m,1H), 0.50(m,3H)	189.9(m,1C), 179.9 (bs,1C)
[RhIr(CH$_3$)(CO)$_2$(PPhMe$_2$)(dppm)$_2$][CF$_3$SO$_3$] (**4c**)[f]	1958(bs)	13.7(dm,$^1J_{RhP}$=130Hz), 6.0(dm, $^1J_{RhP}$=131Hz), −24.2(m), −30.5(m), −45.3(m)	5.60(m,1H), 4.97(m,1H), 4.78(m,1H), 4.70(m,1H), 0.52(d,3H), 0.48(d,3H), 0.44(dt,3H)	182.4(dm,$^1J_{RhC}$=70Hz,1C), 179.9(bs,1C)
[RhIr(CH$_3$)(CO)$_2$(PPh(OMe)$_2$)(dppm)$_2$][CF$_3$SO$_3$] (**4d**)[f]	1957(bs)	117.4(m), 17.2(dm,$^1J_{RhP}$=157Hz), 9.6(dm,$^1J_{RhP}$=129Hz), −22.1(m), −23.7(m)	5.17(m,1H), 4.90(m,1H), 4.55(m,1H), 4.45(m,1H), 3.32(d,3H), 3.16(d,3H), −0.18(dt,3H)	182.5(bs,1C), 181.8(dm,$^1J_{RhC}$=73Hz)
[RhIr(CH$_3$)(μ-CO)(PMe$_3$)(dppm)$_2$][CF$_3$SO$_3$] (**5a**)	1953(ss), 1747(sb)[c]	25.8(ddm,$^1J_{RhP}$=132Hz, $^2J_{PP}$=42Hz), 18.3(m), −32.6(dt,$^1J_{RhP}$=138Hz)	4.22(m,2H), 3.41(m,2H), 0.35(td, $^3J_{PH}$=6Hz,$^4J_{PH}$=2Hz,3H), 0.28(dd, $^2J_{PH}$=8Hz,$^3J_{RhH}$=1Hz,9H)	214.5(ddm,$^1J_{RhC}$=36Hz, $^2J_{PC}$=27Hz,1C)
[RhIr(CH$_3$)(μ-CO)(PPhMe$_2$)(dppm)$_2$][CF$_3$SO$_3$] (**5c**)	1774(ss)[c]	24.1(ddm,$^1J_{RhP}$=130Hz, $^2J_{PP}$=41Hz), 15.2(m), −19.2($^1J_{RhP}$=143Hz,$^4J_{PP}$=6Hz)	4.48(m,2H),3.65(m,2H), 0.47(td,3H), 0.60(d,6H)	212.2(ddm,$^1J_{RhC}$=36Hz, $^2J_{PC}$=26Hz,1C)
[RhIr(CH$_3$)(CN)(CO)$_2$(dppm)$_2$] (**6**)	2084(m),[e] 1960(m), 1932(ss)	11.4(dm,$^1J_{RhP}$=146Hz), −18.2(m)	5.84(m,2H), 5.38(m,2H), −0.74(t,3H)	187.2(t,1C), 183.8(dt,$^1J_{RhC}$=67Hz,1C)
[RhIr(CH$_3$)(H)(CO)$_2$(dppm)$_2$] (**7**)[f]		15.8(dm,$^1J_{RhP}$=147Hz), −7.2(m)	5.22(m,4H), −1.02(t,3H), −10.08(t,1H)	182.4(dt,$^1J_{RhC}$=83Hz,1C), 190.4(bs,1C)
[RhIr(H)(CO)$_2$(μ_2-h$_3$-(-o-C$_6$H$_4$PPh-CH$_2$PPh$_2$))(dppm)] (**8**)		6.7 and 5.6(complex multiplet), −18.6(m), −33.7(m)	5.36(m,1H), 5.02(m,1H), 4.18(m,1H), 4.08(m,1H), −11.93(bm, $^1J_{RhH}$=5Hz,1H)	187.4(dm,$^1J_{RhC}$=74Hz,1C), 174.2(bs,1C)
[RhIr(CH$_3$)(I)(CO)$_2$(dppm)$_2$] (**9**)	1931(ss), 1761(m)	33.8(dm,$^1J_{RhP}$=152Hz), −4.1(m)	4.48(m,2H), 4.22(m,2H), −0.63(td,3H)	212.3(dm,$^1J_{RhC}$=40Hz,1CO), 179.7(m,1CO), 3.1 (dt,$^1J_{RhC}$=22Hz,1C)

[a] IR abbreviations: ss = strong sharp, sb = strong broad, ms = medium sharp, m = medium, w = weak, sh = shoulder. NMR abbreviations: t = triplet, d = doublet, dt = doublet of triplets, dd = doublet of doublets, tt = triplet of triplets, ddt = doublet of doublets of triplets, ddm = doublet of doublets of multiplets, dm = doublet of multiplets, td = triplet of doublets, bs = broad singlet, m = multiplet, q = quartet, s = singlet. [b] Nujol mull except as indicated. Values quoted are ν(CO) except as indicated. [c] CH_2Cl_2 cast. [d] ^{31}P{^{1}H} chemical shifts are referenced vs external 85% H_3PO_4 while ^{1}H and ^{13}C{^{1}H} are referenced vs TMS. Chemical shifts for the phenyl hydrogens are not given in the ^{1}H NMR data. [e] ν(CN) for CN. [f] NMR spectra at −40 °C. [g] NMR spectra at −60 °C.

Table 2. Crystallographic Experimental Details for Compounds 2 and 4a

	2	**4a**·2THF
	A. Crystal Data	
formula	$C_{54}H_{47}F_3IrO_5P_4RhS$	$C_{65}H_{72}F_3IrO_7P_5RhS$
fw	1283.97	1504.25
cryst dimers (mm)	0.62 × 0.42 × 0.24	0.36 × 0.21 × 0.08
cryst syst	monoclinic	monoclinic
space group	$P2_1/n$ (a nonstandard setting of $P2_1/c$ [No. 14])	$P2_1/n$
unit cell params		
a (Å)	13.858(1)	16.431(2)
b (Å)	15.637(1)	23.117(3)
c (Å)	23.671(1)	17.851(2)
β (deg)	96.525(6)	93.41(1)
V (Å^3)	5096.1(7)	6768(1)
Z	4	4
ρ_{calcd} (g cm^{-3})	1.673	1.476
μ (mm^{-1})	9.661	2.414
	B. Data Collection and Refinement Conditions	
diffractometer	Siemens P4/RA[a]	Enraf-Nonius CAD4[d]
radiation [l (Å)]	graphite-monochromated Cu Kα (1.541 78)	graphite-monochromated Mo Kα (0.710 73)
temp (°C)	−60	−50
scan type	$\theta-2\theta$	$\theta-2\theta$
data collcn 2θ limit (deg)	115.0	50.0
total no. of data collcd	7133 ($0 \le h \le 15$, $0 \le k \le 17$, $-23 \le l \le 23$)	12 274 ($-19 \le h \le 19$, $0 \le k \le 27$, $0 \le l \le 21$)
no. of ind reflns	6817	11867
no. of obs (NO)	6119 ($F_o^2 \ge 2\sigma(F_o^2)$)	4211 ($F_o^2 \ge 2\sigma(F_o^2)$)
structure solution method	direct methods/fragment search (DIRDIF-96)	direct methods (SHELXS-86)
refinement method	full-matrix least-squares on F^2 (SHELXL-93)	full-matrix least-squares on F^2 (SHELXL-93)
abs corr method	semiempirical (ψ scans)	DIFABS[e]
range transm factors	0.9595−0.1741	1.217−0.619
no. of data/restraints/params	6815 [$F_o^2 \ge -3\sigma(F_o^2)$]/0/630	11858 [$F_o^2 \ge -3\sigma(F_o^2)$]/39[f]/647
goodness-of-fit (S)[b]	1.087 [$F_o^2 \ge -3\sigma(F_o^2)$]	0.998 [$F_o^2 \ge -3\sigma(F_o^2)$]
final R indices[c]		
R_1 [$F_o^2 \ge 2\sigma(F_o^2)$]	0.0726	0.0915
wR_2 [$F_o^2 \ge -3\sigma(F_o^2)$]	0.1980	0.3249
largest diff peak and hole (e Å)$^{-3}$	2.474 and −3.664	1.761 and −2.362

[a] Programs for diffractometer operation, data collection, data reduction, and absorption correction were those supplied by Siemens. [b] $S = [\sum w(F_o^2 - F_c^2)^2/(n-p)]^{1/2}$ (n = number of data; p = number of parameters varied; $w = [\sigma^2(F_o^2) + (a_oP)^2 + a_1P]^{-1}$ where $P = [\max(F_o^2, 0) + 2F_c^2]/3$).[6] [c] $R_1 = \sum(||F_o| - |F_c||)/\sum|F_o|$; $wR_2 = \sum w(F_o^2 - F_c^2)^2/\sum w(F_o^4)]^{1/2}$. [d] Programs for diffractometer operation and data collection were those supplied by Enraf-Nonius. [e] See ref 7. [f] Restraints were applied to fix the geometries of the triflate group (S−C91 = 1.80 Å; S−O91 = S−O92 = S−O93 = 1.45 Å, F91−C91 = F92−C91 = F93−C91 = 1.35 Å; F91−F92 = F91−F93 = F92−F93 = 2.20 Å; O91−O92 = O91−O93 = O92−O93 = 2.20 Å; F91−O91 = F91−O92 = F92−O91 = F92−O93 = F93−O92 = F93−O93 = 3.04 Å) and the THF rings (all bond distances 1.50 Å; all 1,3 distances [e.g. C101−C103] 2.45 Å).

Downloaded by CARLI CONSORTIUM on June 30, 2009
Published on April 8, 1999 on http://pubs.acs.org | doi: 10.1021/om980947y

Several crystals were mounted and flame-sealed in glass capillaries under solvent vapor to minimize decomposition or deterioration due to solvent loss. Unit cell parameters (at −60 °C) were obtained from a least-squares refinement of 33 reflections in the approximate range 57.0° < 2θ < 58.0°. The cell parameters and systematic absences ($h0l$, $h+l$ = odd, $0k0$, k = odd) defined the space group $P2_1/n$. Data were collected at −60 °C on a Siemens P4RA diffractometer using graphite-monochromated Cu Kα radiation, employing a $\theta/2\theta$ scan technique to a maximum 2θ = 115.0°. Backgrounds were scanned for 25% of peak width on either side of the peak scan. Of 7133 unique reflections, 6119 were considered to be observed [$F_o^2 \ge 3\sigma(F_o^2)$] and were used in subsequent calculations. Absorption correction to **2** was by semiempirical method using ψ scans. Crystal parameters and details of data collection are given in Table 2.

X-ray Data Collection for [RhIr(CH$_3$)(CO)$_2$(PMe$_3$)(dppm)$_2$][CF$_3$SO$_3$] (4a)·2THF. Diffusion of ether into a concentrated THF solution of **4a** yielded yellow crystals of the complex, several of which were mounted and flame-sealed in glass capillaries under solvent vapor to minimize decomposition and (or) solvent loss. Data were collected at −50 °C on an Enraf-Nonius CAD4 diffractometer using graphite-monochromated Mo Kα radiation. Unit cell parameters were obtained from a least-squares refinement of the setting angles of 24 reflections in the range 20.0° < 2θ < 23.9°. The monoclinic diffraction symmetry and systematic absences ($h0l$, $h+l$ = odd, $0k0$, k = odd) were consistent with the space group $P2_1/n$. Intensity data were collected using the $\theta/2\theta$ scan technique to a maximum 2θ = 50.0°. Of 11 867 unique reflections, 4211 were considered to be observed [$F_o^2 \ge 3\sigma(F_o^2)$] and were used in subsequent calculations. Absorption corrections were applied to the data using the method of Walker and Stuart.[7,8] Crystal parameters and details of data collection are given in Table 2.

Structure Solution and Refinement for Compound 2. The positions of Rh, Ir, and phosphorus atoms were located using direct methods/fragment search program DIRDIF-96;[9] the remaining atoms were found using a succession of least-squares and Fourier maps. Refinement of the structure proceeded using the program SHELXL-93.[10] The hydrogen positions were calculated by assuming idealized sp^2 or sp^3 geometries about their attached carbon atoms as appropriate and were given thermal parameters 120% of the equivalent isotropic displacement parameters of the attached carbons. Initial refinements indicated unusually high thermal parameter for the atoms of the terminal and bridging carbonyls and the methyl carbon atoms. In addition, the isotropic thermal

(6) The coefficients a_o and a_1 in the weighting scheme are suggested by the least-squares refinement program: for **2**, a_o = 0.1404 and a_1 = 22.2339; for **4a**·2THF, a_o = 0.1435 and a_1 = 0.

(7) Walker, N.; Stuart, D. *Acta Crystallogr., Sect A: Found Crystallogr.* **1983**, *A39*, 158.

(8) Programs used were those of the Enraf-Nonius Structure Determination Package by B. A. Frenz, in addition to local Programs by R. G. Ball.

(9) Beurskens, P. T.; Beurskens, G.; Bosman, W. P.; de Gelder, R.; Garcia Granda, S.; Gould, R. O.; Israel, R.; Smith, J. M. M. *The DIRDIF-96 program system*; Crystallography Laboratory, University of Nijmegen: The Netherlands, 1996.

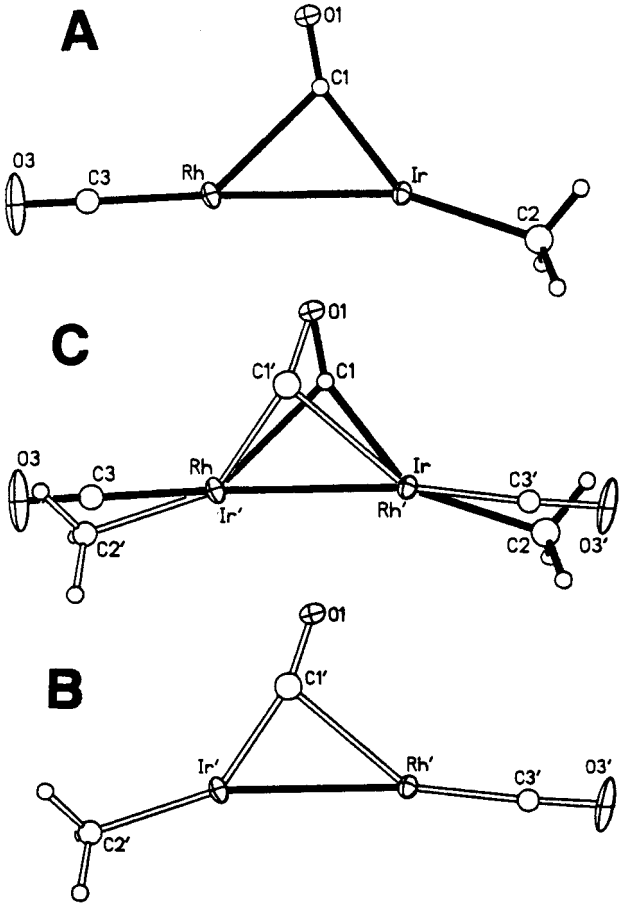

Figure 1. Illustration of the disorder within the "RhIr(CH$_3$)(CO)(μ-CO)" unit of compound **2**. Drawing **A** shows the orientation of the molecule having 55% occupancy, **B** shows the 45% occupancy molecule, and **C** shows the two superimposed molecules. Unprimed atoms have 55% occupancy (except for O(1), which has 100% occupancy), and primed atoms have 45% occupancy, so the metal position Ir/Rh′ was refined with a mixed occupancy of 55% iridium and 45% rhodium.

parameter for Ir was unusually high while that of Rh was unusually low. This suggested a rotational disorder in which there are two superimposed orientations for the complex as depicted in Figure 1 (dppm ligands omitted for clarity). The disorder of the terminal carbonyl group attached to Rh was suggested by the extreme elongation of the thermal ellipsoids of C(3) and O(3) in a direction perpendicular to the Rh−C(3) bond axis. Subsequent difference Fourier maps indicated that the disordered methyl and carbonyl carbons were not exactly superimposed (with the exception of the oxygen atom O(1) of the bridging carbonyl, which was shared between the two disordered molecules and was refined at full occupancy) but were slightly offset from each other. This together with the anomalous thermal parameters for the metals led to the model shown in which the two orientations **A** and **B** are disordered in approximately a 55:45 ratio (determined from the relative peak intensities of the ordered and disordered atoms), to give the average structure **C**, having the weightings in which the unprimed atoms shown in Figure 1 have 55% occupancy (except for O(1)) and the primed ones have 45% occupancy. The solid bonds in **C** connect atoms of the major occupant, while the open bonds connect atoms of the minor occupant. Due to the disorder there will be some degree of uncertainty about the bond distances involving the disordered atoms; however the gross structure is clearly established. In addition, the bridging mode of the carbonyl group in the solid state was established by solid-state ^{13}C NMR spectral results (vide infra). A similar disorder has been observed in the X-ray structure analyses for [RhIr(CH$_3$)(CO)$_3$(dppm)$_2$][CF$_3$SO$_3$],[2b] [Ir$_2$(CH$_3$)(CO)$_2$(dppm)$_2$][[CF$_3$SO$_3$],[1b] [RhMn(CO)$_3$(μ-CO$_3$)(dppm)$_2$],[11] and [RhM(CO)$_4$(dppm)$_2$] (M = Mn, Re).[12] Location of the dppm atoms in **2** proceeded well with no evidence of disorder.

Structure Solution and Refinement for compound 4a. The positions of the Rh, Ir, and phosphorus atoms were obtained through use of the direct-methods program SHELXS-86.[13] The remaining non-hydrogen atoms were located using successive least-squares and difference Fourier maps. All hydrogen atoms with the exception of the THF hydrogens were included as fixed contributions but not refined. Their idealized positions were calculated from the geometries about the attached carbon atoms, using a C−H bond length of 0.95 Å, and they were assigned thermal parameters 20% greater than the equivalent isotropic *U*'s of their attached carbon atoms. Refinement was completed using the program SHELXL-93.[10] All non-hydrogen atoms of the complex cation and anion were located. In addition, two molecules of THF per formula unit of complex were also located.

Results and Compound Characterization

The heterobinuclear methyl complex [RhIr(CH$_3$)(CO)$_3$(dppm)$_2$][CF$_3$SO$_3$] (**1**) has previously been characterized[2] and has been shown to have the geometry depicted in Scheme 1, in which the methyl group is terminally bound to iridium in the site opposite the Rh−Ir bond. This species is static on the NMR time scale at ambient temperature and shows no evidence of carbonyl exchange between the metals or transfer of the methyl group from metal to metal as occurs readily in the dicarbonyl analogues of Rh$_2$[14] and Ir$_2$.[1] The exact analogue of these homobimetallic, dicarbonyl complexes can be generated through CO loss from **1** by refluxing in CH$_2$Cl$_2$ to give [RhIr(CH$_3$)(CO)$_2$(dppm)$_2$][CF$_3$SO$_3$] (**2**). Based on previous work, two structures seemed possible for **2** in the solid state, having the methyl group either terminally bound to one metal, as in the solid-state structures of [M$_2$(CH$_3$)(CO)(μ-CO)(dppm)$_2$][CF$_3$SO$_3$] (M = Rh,[14] Ir[1]), or bridging the metals as in the dmpm analogue [Ir$_2$(CO)$_2$(μ-CH$_3$)(dmpm)$_2$][CF$_3$SO$_3$] (dmpm = Me$_2$PCH$_2$PMe$_2$).[15] The IR spectrum of **2** in the solid indicates that one carbonyl is terminal (1997 cm^{-1}) and one is bridging (1858 cm^{-1}). The CP-MAS ^{13}C NMR spectra of ^{13}CO- and ^{13}CH$_3$-enriched samples of **2** were undertaken in order to help establish its solid-state structure. A broad (54 Hz at peak half-height) overlapping pair of doublets, each displaying coupling to Rh of 80 Hz, appear at δ 177.0 and δ 176.0 for the Rh-bound carbonyl. The observation of two resonances is consistent with the disorder of **2** in the solid state (see

(10) Sheldrick, G. M. *SHELXL-93*. Program for crystal structure determination; University of Gottingen, Gottengen, Germany, 1993. Refinement on F_o^2 for all reflections (all of those having $F_o^2 > -3\sigma(F_o^2)$). Weighted *R* factors wR2 and all goodness of fit are based on F_o^2; conventional *R* factors R1 are based on F_o, with F_o set to zero for negative F_o's. The observed criterion of $F_o^2 > -2\sigma(F_o^2)$ is used only for calculating R1 and is not relevant to the choice of reflections for refinement. *R* factors based on F_o^2 are statistically about twice as large as those based on F_o, and *R* factors based on ALL data be even larger.

(11) Antonelli, D. M.; Cowie, M. *Organometallics* **1991**, *10*, 2173.
(12) Antonelli, D. M.; Cowie, M. *Organometallics* **1990**, *9*, 1818.
(13) Sheldrich, G. M. *Acta Crystallogr.* **1990**, *A46*, 467.
(14) Shafiq, F.; Kramarz, K. W.; Eisenberg, R. *Inorg. Chim. Acta* **1993**, *213*, 111.
(15) Reinking, M. K.; Fanwick, P. E.; Kubiak, C. P. *Angew. Chem., Int. Ed. Engl.* **1989**, *20*, 1377.

Downloaded by CARLI CONSORTIUM on June 30, 2009
Published on April 8, 1999 on http://pubs.acs.org | doi: 10.1021/om980947y

Scheme 1

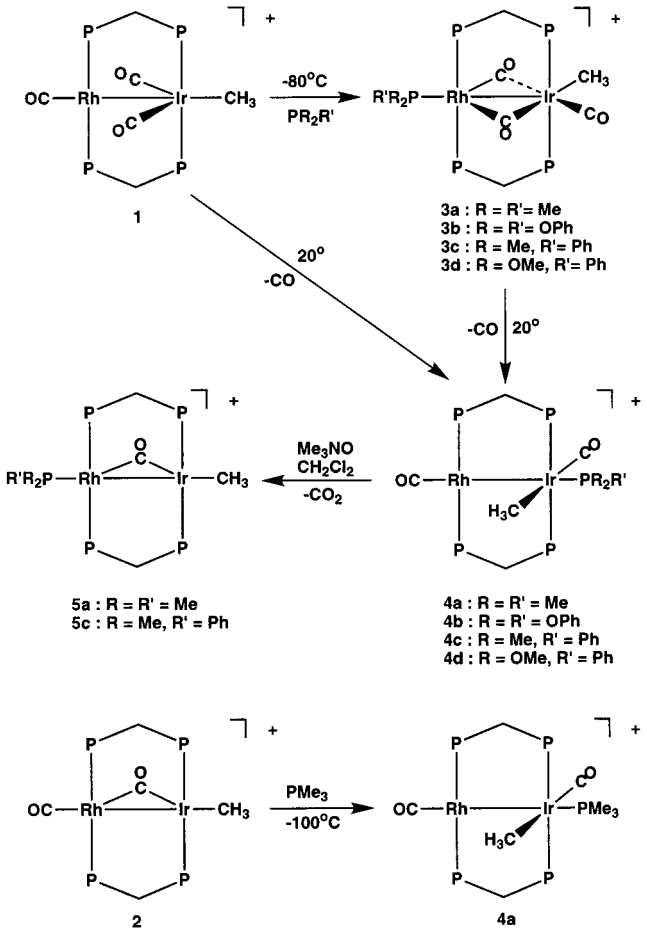

Experimental Section) in which there are two orientations of the complex and therefore two environments for each carbonyl. The second carbonyl resonance appears at δ 193.0, in a downfield position consistent with a bridging arrangement; however, the breadth of this resonance (140 Hz) does not allow us to determine the magnitude of the coupling to Rh. Presumably the breadth of this resonance also masks the two environments anticipated for this carbonyl owing to the disorder. The resonance for the methyl group, at δ 14.8, is far too broad (ca. 450 Hz) to display any useful coupling information. The location of the terminal carbonyl on Rh, rather than on Ir, is further supported by its stretching frequency, which is 23 cm^{-1} higher than in the Ir_2 analogue,[1] but close to the value of 2007 cm^{-1} observed in the Rh_2 species.[14] The possibility of the triflate anion being coordinated to either metal is ruled out by its IR spectrum, which shows stretches at 1226, 1257, and 1281 cm^{-1}, consistent with the uncomplexed ion.[16] As such, the structure of **2**, diagrammed in Scheme 1, resembles the two homobinuclear, dppm-bridged analogues, having a terminal methyl group and a bridging carbonyl.

An X-ray structure determination of **2** was undertaken in order to confirm the above bonding proposal and to determine the asymmetry in the binding of the bridging carbonyl. Unfortunately, owing to a 55:45 disorder, as described in the Experimental Section, a detailed bonding picture cannot be established solely

(16) Stang, P. J.; Cao, D. *Organometallics* **1993**, *12*, 996.

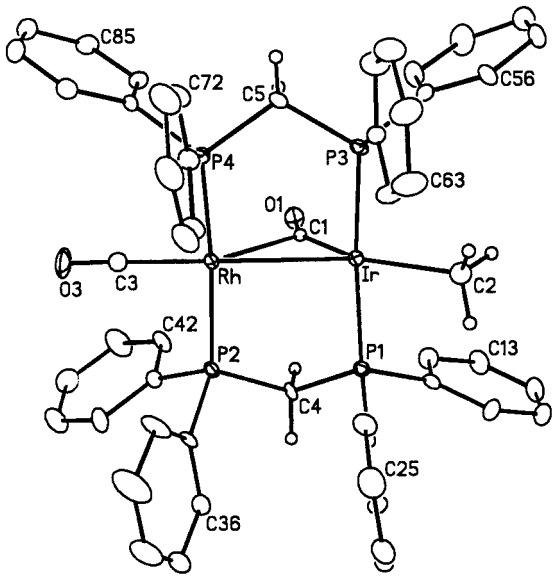

Figure 2. Perspective view of the $[RhIr(CH_3)(CO)(\mu\text{-}CO)(dppm)_2]^+$ complex ion of **2**, showing the atom-labeling scheme (only the major contributor to the disorder is shown). Non-hydrogen atoms are shown with 20% thermal ellipsoids; hydrogen atoms are shown with arbitrarily small thermal parameters apart for those on the phenyl groups, which are not shown.

from the X-ray results. However, the structure shown in Figure 2 is consistent with all spectroscopic data in the solid state (vide supra), and together these data leave little doubt about the structure. Clearly one carbonyl bridges the metals, and despite the disorder, its semibridging nature, being more closely associated with Ir than Rh, is established. The asymmetry in the binding of the bridging carbonyl is obvious from the parameters shown in Table 3, in which the Ir−C(1) bond (1.99(2), 1.88(3) Å for the two disordered units) is substantially shorter than the Rh−C(1) distance (2.28(2), 2.34(3) Å). This carbonyl is correspondingly more linear with respect to Ir (Ir−C(1)−O(1) 153(2)°, 164(3)°; Rh−C(1)−O(1) 124(2)°, 112(2)°). The asymmetry in this carbonyl is in contrast to the essentially symmetrically bridged carbonyl in the Rh_2 and Ir_2 analogues, and the stronger binding of this bridging carbonyl to Ir is not unexpected. This asymmetry is also reflected in the carbonyl stretch (1858 cm^{-1}), which is higher than both the Rh_2 (1851 cm^{-1}) and Ir_2 (1832 cm^{-1}) analogues, reflecting a slight tendency toward a terminal coordination in the mixed-metal species. All other parameters for compound **2** are in close agreement with those for the Rh_2 and Ir_2 analogues, and in particular the terminal carbonyl is almost along the metal−metal axis in all structures (M−M−CO angles: $M_2 = Rh_2$, av 176°; Ir_2, av 177°; RhIr, av 175°), while the methyl group is significantly off this axis (M−M−CH_3 angles: $M_2 = Rh_2$, av 161°; Ir_2, av 164°; RhIr, av 162°).

In solution the structure of **2** is somewhat different than in the solid state. This is most evident from the solution IR spectrum, which shows no bridging carbonyl stretch and exhibits only one broad carbonyl band at 1954 cm^{-1}; this band presumably is a combination of the stretches for the terminal carbonyls on Rh and Ir. The $^{13}C\{^1H\}$ NMR spectrum of **2** in solution shows one carbonyl resonance at δ 175.4 with coupling of 73 Hz to Rh and smaller coupling to the Rh-bound phosphines,

Downloaded by CARLI CONSORTIUM on June 30, 2009
Published on April 8, 1999 on http://pubs.acs.org | doi: 10.1021/om980947y

Table 3. Selected Bond Lengths and Angles for [RhIr(CH$_3$)(CO)(μ-CO)(dppm)$_2$][CF$_3$SO$_3$] (2)[a]

Selected Interatomic Distances (Å)			
Ir−Rh	2.8290(7)	Rh′−C(1′)	2.34(3)
Ir/Rh′−P(1)	2.317(2)	Rh′−C(3′)	1.79(2)
Ir/Rh′−P(3)	2.319(2)	P(1)−C(4)	1.837(9)
Ir−C(1)	1.99(2)	P(2)−C(4)	1.826(9)
Ir−C(2)	2.14(3)	P(3)−C(5)	1.820(10)
Ir′−C(1′)	1.88(3)	P(4)−C(5)	1.830(9)
Ir′−C(2′)	2.03(3)	O(1)−C(1)	1.07(2)
Rh/Ir′−P(2)	2.311(2)	O(1)−C(1′)	1.16(3)
Rh/Ir′−P(4)	2.310(3)	O(3)−C(3)	1.07(3)
Rh−C(1)	2.28(2)	O(3′)−C(3′)	1.13(3)
Rh−C(3)	1.84(2)		

Selected Interatomic Angles (deg)			
Rh/Ir′−Ir/Rh′−P(1)	91.15(6)	P(4)−Rh−C(1)	97.8(4)
Rh/Ir′−Ir/Rh′−P(3)	93.15(6)	P(4)−Rh−C(3)	87.3(6)
Rh−Ir−C(1)	53.1(6)	C(1)−Rh−C(3)	138.1(9)
Rh−Ir−C(2)	161.0(7)	Ir′−Rh′−C(1′)	41.3(8)
P(1)−Ir/Rh′−P(3)	173.57(8)	Ir′−Rh′−C(3′)	172.7(9)
P(1)−Ir−C(1)	90.4(5)	P(1)−Rh′−C(1′)	91.5(7)
P(1)−Ir−C(2)	85.7(7)	P(1)−Rh′−C(3′)	88.1(8)
P(3)−Ir−C(1)	96.0(5)	P(3)−Rh′−C(1′)	94.8(7)
P(3)−Ir−C(2)	88.7(7)	P(3)−Rh′−C(3′)	87.0(8)
C(1)−Ir−C(2)	145.5(9)	C(1′)−Rh′−C(3′)	146.0(12)
Rh′−Ir′−C(1′)	55.4(9)	Ir/Rh′−P(1)−C(4)	113.7(3)
Rh′−Ir′−C(2′)	162.4(8)	Rh/Ir′−P(2)−C(4)	113.2(3)
P(2)−Ir′−C(1′)	91.1(8)	Ir/Rh′−P(3)−C(5)	113.0(3)
P(2)−Ir′−C(2′)	87.5(7)	Rh/Ir′−P(4)−C(5)	113.1(3)
P(4)−Ir′−C(1′)	97.9(8)	Ir−C(1)−Rh	82.7(6)
P(4)−Ir′−C(2′)	86.4(7)	Ir−C(1)−O(1)	153.2(16)
C(1′)−Ir′−C(2′)	142.2(13)	Rh−C(1)−O(1)	123.9(15)
Ir/Rh′−Rh/Ir′−P(2)	92.92(6)	Ir′−C(1′)−Rh′	83.4(10)
Ir/Rh′−Rh/Ir′−P(4)	90.76(6)	Ir′−C(1′)−O(1)	164.3(26)
Ir−Rh−C(1)	44.2(5)	Rh′−C(1′)−O(1)	112.3(22)
Ir−Rh−C(3)	177.2(7)	Rh−C(3)−O(3)	178.9(19)
P(2)−Rh/Ir′−P(4)	170.77(8)	Rh′−C(3′)−O(3′)	176.3(30)
P(2)−Rh−C(1)	90.7(4)	P(1)−C(4)−P(2)	109.7(5)
P(2)−Rh−C(3)	88.7(6)	P(3)−C(5)−P(4)	110.3(5)

[a] Primed and unprimed atoms are related by a 55:45 disorder. See Figure 1 for an explanation of labeling.

and another at 184.9 as a broad resonance. Resolution enhancement of this latter resonance gives a doublet with coupling to Rh of 7 Hz. The $^{13}C\{^1H\}$ NMR spectrum of a $^{13}CH_3$-enriched sample shows the methyl resonance as a triplet at δ 17.8, and the ^1H NMR (unenriched sample) shows a triplet at δ 0.59, with only ^{31}P coupling observed in both cases. The absence of Rh coupling clearly establishes that the methyl group is bound to Ir. These spectroscopic data mirror the spectral changes between solid and solution that were observed for the diiridium analogue. We therefore propose a structure for **2** in solution as shown below (labeled **2a**), much like that proposed in the Ir_2 complex.[1b]

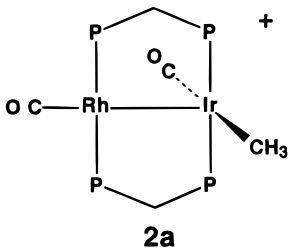

2a

In **2a** the slight (7 Hz) coupling to Rh either could result from two-bond coupling through the Rh−Ir bond or could arise from a very weak semibridging carbonyl interaction. We favor the latter formulation since we have seen no other examples in our extensive chemistry of mixed RhM (M = Ru,[17] Os,[18] Ir,[19] Mn,[20] Re,[21] Mo,[22] W[22]) complexes in which Rh coupling was observed in a carbonyl bound to the adjacent metal, unless involved in some form of bridging interaction with Rh. Furthermore, the $^{13}C\{^1H\}$ chemical shift of this primarily Ir-bound carbonyl is at lower field than that for the carbonyl on Rh, opposite to what is expected,[23] suggesting a weak semibridging interaction.[24] In further support of this formulation, DFT calculations on the Ir_2 analogue $[Ir_2(CH_3)(CO)_2(H_2PCH_2PH_2)_2]^+$ (phenyl groups on dppm substituted by hydrogens to facilitate calculations) independently arrived at the same structure and also indicated that the carbonyl trans to CH_3 was tipped in slightly toward the adjacent metal,[1b] presumably reflecting a weak interaction with it. It should be emphasized that the NMR spectra of **2** in the solid and in solution are only subtly different, reflecting the subtle structural change in which the semibridging carbonyl moves slightly away from Rh, accompanied by movement of the methyl group off the Rh−Ir axis.

Unlike the Rh_2 and Ir_2 analogues, which are fluxional in solution, with carbonyl and methyl groups migrating readily from metal to metal, compound **2**, like its tricarbonyl precursor (**1**), is static at ambient temperature. Presumably the stronger Ir−CO and Ir−CH_3 bonds[25] inhibit migration to Rh.

Compounds **1** and **2** have been reacted with a number of nucleophiles in order to determine the sites of attack in both compounds, the rearrangements of added substrate and the methyl group that may occur, and whether a bridging methyl group could be observed that would model the C−H bond-activation process in the Ir_2 analogues. We first looked at the reactivity of **1** and **2** with phosphines; the reactions of **1** with ^{t}BuNC, SO_2, and ethylene have already been reported.[2b] Compound **1** reacts with the phosphines (PMe_3, PMe_2Ph, $P(OMe)_2Ph$, and $P(OPh)_3$) at ambient temperature with accompanying CO loss to yield the products $[RhIr(CH_3)(PR_2R')(CO)_2(dppm)_2][CF_3SO_3]$ (**4**), having the added phosphine and the methyl group bound to Ir, as shown in Scheme 1. Although this reaction proceeded smoothly with the phosphines listed, no reaction was observed with PPh_3, even after prolonged reaction times, presumably due to restricted approach of this bulky substrate by interactions with the phenyl groups of the dppm ligands. At ambient temperature the $^{31}P\{^1H\}$ NMR spectra of all species display three broad unresolved resonances in a 2:2:1 intensity ratio, whereas at −40 °C these spectra transform to complicated patterns of five resonances

Downloaded by CARLI CONSORTIUM on June 30, 2009
Published on April 8, 1999 on http://pubs.acs.org | doi: 10.1021/om980947y

(17) Sterenberg, B. T. Ph.D. Thesis, University of Alberta, 1997, Chapter 5.
(18) (a) Sterenberg, B. T.; Hilts, R. W.; Moro, G.; McDonald, R.; Cowie, M. *J. Am. Chem. Soc.* **1995**, *117*, 245. (b) Sterenberg, B. T.; McDonald, R.; Cowie, M. *Organometallics* **1997**, *16*, 2297.
(19) (a) Vaartstra, B. A.; Cowie, M. *Inorg. Chem.* **1989**, *28*, 3138. (b) George, D. S. A.; McDonald, R.; Cowie, M. *Can. J. Chem.* **1996**, *74*, 2289. (c) George, D. S. A.; McDonald, R.; Cowie, M. *Organometallics* **1998**, *17*, 2553.
(20) (a) Wang, L.-S.; McDonald, R.; Cowie, M. *Inorg. Chem.* **1994**, *33*, 3735. (b) Wang, L.-S., Cowie, M. *Can. J. Chem.* **1995**, *73*, 1058. (c) Wang, L.-S., Cowie, M. *Organometallics* **1995**, *14*, 2374.
(21) (a) Antonelli, D. M.; Cowie, M. *Organometallics* **1991**, *10*, 2550. (b) Antonelli, D. M.; Cowie, M. *Inorg. Chem.* **1990**, *29*, 4039.
(22) Graham, T. W.; Van Gastel, F.; McDonald, R.; Cowie, M. *Organometallics*, in press.
(23) Mann, B. E.; Taylor, B. F. *^{13}C NMR Data for Organometallic Compounds*; Academic Press: New York, 1981; p 14.
(24) Adams, H.; Chen, X.; Mann, B. E. *J. Chem. Soc., Dalton Trans.* **1996**, 2159.

consistent with an ABCDMX spin system (X = Rh) in which each phosphorus nucleus is chemically distinct. Taking the spectrum of **4a** as an example, the dppm ^{31}P resonances appear in the expected regions, with those bound to Rh displaying the normal coupling to this nucleus (between 123 and 157 Hz in compounds **4a**−**d**), while the PMe_3 resonance appears as a multiplet at δ −62.4. Appropriate decoupling experiments establish that this group displays coupling to Rh of 17 Hz and to the two phosphorus nuclei on Rh of 15 Hz; no coupling is observed between the PMe_3 group and the dppm phosphorus nuclei bound to Ir. Although the observed $^{31}P-^{31}P$ coupling suggests that the PMe_3 group is bound to Rh, the coupling to this metal is far too small to correspond to $^1J_{Rh-P}$, so the PMe_3 group is assumed to be bound to Ir in the site opposite the Rh−Ir bond. Strong coupling through a metal−metal bond has been observed previously.[5,26] Although we have not observed situations in which a group is coupled to the dppm phosphines on an adjacent metal and not to those on the same metal, we have previously observed a related example, $[IrRu(CO)_3(PMe_3)(\mu\text{-}CH_2)(dppm)_2][BF_4]$,[27] in which the PMe_3 group, shown to be terminally bound to one metal, did display substantial coupling (ca. 9 Hz) to the dppm phosphorus nuclei on the adjacent metal. In this case, however, coupling between PMe_3 and the dppm phosphorus nuclei on the same metal was also observed.

In the ^1H NMR spectrum the methyl ligand appears as a doublet of triplets at δ 0.33 while the PMe_3 protons appear as a doublet at δ 0.23. Selective ^{31}P-decoupling experiments indicate that all coupling to the methyl ligand results from the Ir-bound phosphines, and this, together with the lack of Rh coupling, indicates that it is bound to Ir.

To confirm the geometry proposed for these phosphine adducts, particularly in light of the unusual $^{31}P\{^1H\}$ NMR results, the X-ray structure of **4a** was determined. A perspective view of the cation of **4a** is shown in Figure 3, with relevant bond lengths and angles presented in Table 4. This structure determination confirms the formulation proposed in which the PMe_3 group is coordinated to Ir, in the site opposite the metal−metal bond, and the methyl group is also bound to Ir, opposite the carbonyl ligand. The geometry at Rh is square planar, while that at Ir is distorted octahedral (considering the Rh−Ir bond as occupying one site in each case). Distortions from idealized octahedral geometry about Ir result from repulsions between the PMe_3 group and the adjacent ends of the dppm ligands, as shown by the P(1)−Ir−P(3) angle (157.3(2)°), which deviates substantially from the idealized 180°. Figure 3 shows the close contacts between the PMe_3 group and the dppm phenyl groups 1 and 6, with the resulting geometry at P(1) and P(3) being skewed, forcing rings 2 and 5 toward the Rh end of the molecule. The slightly longer

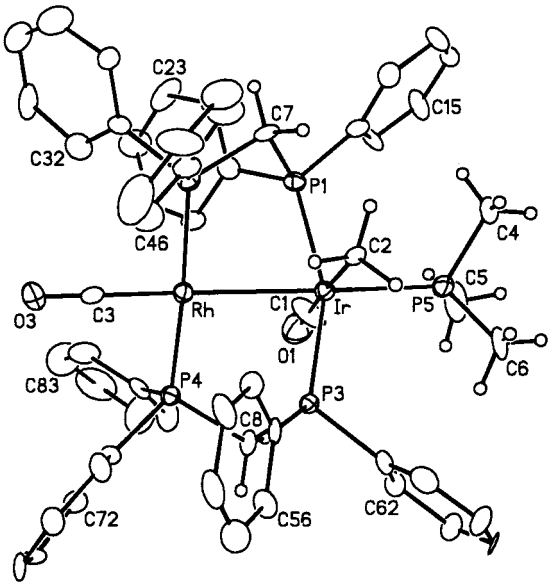

Figure 3. Perspective view of the $[RhIr(CH_3)(CO)_2(PMe_3)(dppm)_2]^+$ complex ion of **4a** showing the atom labeling. Thermal parameters as for Figure 2.

Table 4. Selected Bond Lengths and Angles for $[RhIr(CO)_2(CH_3)(PMe_3)(dppm)_2][CF_3SO_3]\cdot 2C_4H_8O$ (4a)

Selected Interatomic Distances (Å)			
Ir−Rh	2.859(2)	P1−C7	1.81(2)
Ir−P1	2.331(7)	P2−C7	1.84(2)
Ir−P3	2.328(6)	P3−C8	1.87(2)
Ir−P5	2.414(7)	P4−C8	1.85(2)
Ir−C1	1.85(3)	P5−C4	1.77(2)
Ir−C2	2.31(3)	P5−C5	1.79(3)
Rh−P2	2.320(7)	P5−C6	1.71(3)
Rh−P4	2.299(6)	O1−C1	1.14(3)
Rh−C3	1.83(3)	O3−C3	1.13(3)
Selected Interatomic Angles (deg)			
Rh−Ir−P1	79.2(2)	P2−Rh−C3	87.3(8)
Rh−Ir−P3	78.2(2)	P2−Rh−P4	174.9(2)
Rh−Ir−P5	175.7(2)	P4−Rh−C3	90.3(8)
Rh−Ir−C1	94.1(12)	Ir−P1−C7	110.1(8)
Rh−Ir−C2	90.1(6)	Rh−P2−C7	113.7(7)
P1−Ir−P3	157.3(2)	Ir−P3−C8	110.1(9)
P1−Ir−P5	100.5(2)	Rh−P4−C8	114.1(8)
P1−Ir−C1	88.9(11)	Ir−P5−C4	119.2(8)
P1−Ir−C2	90.2(6)	Ir−P5−C5	112.2(10)
P3−Ir−P5	102.2(2)	Ir−P5−C6	120.9(9)
P3−Ir−C1	90.8(10)	C4−P5−C5	102.3(14)
P3−Ir−C2	91.9(6)	C4−P5−C6	100.4(13)
P5−Ir−C1	90.2(12)	C5−P5−C6	98.5(16)
P5−Ir−C2	85.5(6)	Ir−C1−O1	177.4(30)
C1−Ir−C2	175.4(12)	Rh−C3−O3	174.9(32)
Ir−Rh−P2	91.2(2)	P1−C7−P2	105.4(11)
Ir−Rh−P4	91.7(2)	P3−C8−P4	103.8(12)
Ir−Rh−C3	173.6(10)		

Ir−P (2.331(7), 2.328(6) Å) versus Rh−P (2.320(7), 2.299(6) Å) distances for the dppm groups are probably a reflection of the greater crowding at Ir, whereas the long Ir−PMe_3 bond (2.414(7) Å) may result either from the high trans influence of the metal−metal bond[28] or from repulsions with both dppm ligands bound to Ir. An additional consequence of the crowding in the complex is the twisting of the P(1)−Ir−P(3) unit with respect to P(2)−Rh−P(4) by about 40°, as shown in Figure 4, in which the cation of **4a** is viewed approximately along the Rh−Ir bond. This twisting results in different static environments for P(2) (adjacent to $C(2)H_3$) and P(4) (adjacent to C(1)O(1)). The inequiva-

(25) (a) Ziegler, T.; Tschinke, V. *Bonding Energetics in Organometallic Compounds*; Marks, T. J., Ed.; American Chemical Society: Washington, DC, 1990; Chapter 19. (b) Ziegler, T.; Tschinke, V.; Uresenbach, B. *J. Am. Chem. Soc.* **1987**, *109*, 4825. (c) Shen, J.-K.; Tucker, D. S.; Basolo, F.; Hughes, R. P. *J. Am. Chem. Soc.* **1993**, *115*, 11312.

(26) (a) Antwi-Nsiah, F. H.; Torkelson, J. R.; Cowie, M. *Inorg. Chem. Acta* **1997**, *259*, 213. (b) Mague, J. T. *Organometallics* **1986**, *5*, 918. (c) Brown, M. P.; Fisher, J. R.; Hill, R. H.; Puddephatt, R. J.; Seddon, R. R. *Inorg. Chem.* **1981**, *20*, 2516.

Downloaded by CARLI CONSORTIUM on June 30, 2009
Published on April 8, 1999 on http://pubs.acs.org | doi: 10.1021/om980947y

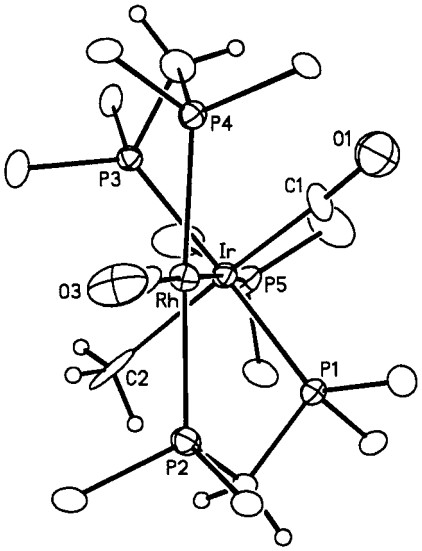

Figure 4. Alternate view of complex **4a**, with all but the ipso carbons of the dppm phenyl rings omitted.

Downloaded by CARLI CONSORTIUM on June 30, 2009
Published on April 8, 1999 on http://pubs.acs.org | doi: 10.1021/om980947y

lence of P(2) and P(4) renders P(1) and P(3) inequivalent and accounts for the different chemical environments of all dppm phosphorus nuclei as observed in the low-temperature $^{31}P\{^1H\}$ NMR spectrum. At ambient temperature, in solution, the molecule is presumably oscillating about the Rh−Ir axis, giving rise to an averaged environment for the ^{31}P nuclei on a given metal, whereas at low temperature the different environments can be detected on the NMR time scale.

We were interested in the initial site of phosphine attack in compound **1**, for which two scenarios seemed possible if the reaction were associative. Either phosphine attack occurs at the unsaturated Rh center, followed by CO loss and migration of the phosphine to Ir, or transfer of a carbonyl from Ir to Rh could occur, followed by phosphine attack directly at Ir and loss of a carbonyl ligand. If the reaction of **1** with phosphines is monitored at −60 °C or lower, the first species observed is the tricarbonyl, phosphine adduct **3** as shown in Scheme 1. Again the spectral parameters for all phosphine adducts are similar, so only those of the PMe_3 adduct (**3a**) are discussed. At −60 °C the $^{31}P\{^1H\}$ NMR spectrum for **3a** shows a resonance for the PMe_3 group as a doublet of triplets at δ −35.4. The coupling of 147 Hz to Rh clearly identifies this group as being directly bound to this metal. Furthermore, it is noteworthy that this resonance is ca. 20 ppm downfield from the PMe_3 resonance in **4a** and parallels the trend in ^{31}P chemical shifts for the dppm resonances in which the Rh end is generally downfield from the Ir end. The $^{13}C\{^1H\}$ NMR spectrum of **3a** shows three equal intensity peaks, one at δ 262.7 ($^1J_{RhC} = 25$ Hz) corresponding to a bridging carbonyl, a second at δ 202.4 ($^1J_{RhC} = 53$ Hz) for the carbonyl on Rh, and a third resonating at δ 185.1, corresponding to a carbonyl which is terminally bound to Ir. The slight downfield shift of the central resonance and the magnitude of its coupling to Rh, which is less than usually observed for a terminal carbonyl, suggests that although primarily bound to Rh, it has a weak semibridging interaction with Ir. The net result of PMe_3 attack at Rh is that one of the two iridium-bound carbonyls of **1** has transferred to the bridging position, while the terminal carbonyl on Rh has adopted a weak semibridging arrangement, although remaining primarily bound to Rh. Movement of a carbonyl from Ir to the bridging site, in which a more crowded environment at Rh results, is not expected based on steric arguments, but probably occurs in order to alleviate some of the buildup of electron density on Rh upon addition of the phosphine. A similar situation has previously been observed in a related diiridium system in which ligand addition at one metal caused a carbonyl on an adjacent metal to move to a bridging site.[29]

Upon warming **3a** to −40 °C peaks due to the dicarbonyl product **4a** begin to appear, and by −20 °C **4a** is the predominant species in solution. Rearrangement accompanied by CO loss results in transfer of the phosphine from Rh to Ir. This may occur either by direct transfer via a phosphine-bridged intermediate or by phosphine loss and subsequent recoordination at the different metal. We have no evidence to support either route. Although no PR_3-bridged complexes are known, phosphine transfer in binuclear systems, via a bridged intermediate, has been suggested.[30,31] In addition, a related trialkylstibane-bridged analogue, $[Rh_2Cl_2(\mu\text{-}SbiPr_3)(\mu\text{-}CPh_2)]$ is known,[32] and the possibility of phosphine-bridged clusters has also been suggested.[33]

In the case of **2**, in which both metals are coordinatively unsaturated, reaction with trimethylphosphine again yields compound **4a**. However in this case attack appears to occur directly at Ir, since no other species is observed at temperatures down to −100 °C.

One carbonyl can be removed from compounds **4a** and **4c** by reaction with Me_3NO, yielding the monocarbonyl products $[RhIr(CH_3)(PR_3)(\mu\text{-}CO)(dppm)_2][CF_3SO_3]$ (**5a** and **5c**), as shown in Scheme 1. Carbonyl loss is accompanied by migration of the monodentate phosphine from Ir back to Rh as seen by the magnitude of the Rh coupling ($^1J_{RhP} = 138$ Hz (spectral parameters for **5a** are discussed)). The methyl group remains bound to Ir as seen by ^1H NMR experiments in which coupling to the Ir-bound dppm phosphorus nuclei ($^3J_{PH} = 6$ Hz) is observed. A slight, additional coupling to the PMe_3 group ($^4J_{PH} = 2$ Hz) is also observed and suggests an alignment of PMe_3 and CH_3 ligands opposite the metal−metal bond as in the related dicarbonyl monomethyl species. In solution the carbonyl is shown both by IR (ν(CO) = 1746 cm^{-1}) and by $^{13}C\{^1H\}$ NMR spectroscopy to be bridging the metals. The ^{13}CO resonance at δ 214.5 is at low field, typical of a bridging group and shows coupling to Rh (36 Hz) and to all five phosphorus nuclei. In the solid state the structure of **5** again differs from that in solution, but now in the opposite way compared to **2**; the IR spectra of **5a** and **5c** in the solid show only a terminal carbonyl band. Clearly packing effects in the solid state induce subtle structural changes favoring a

(27) Dell'Anna, M. M.; Cowie, M. Unpublished results.
(28) (a) Cowie M.; Dwight, S. K. *Inorg. Chem.* **1980**, *19*, 209. (b) Cowie, M.; Gibson, J. A. E. *Organometallics* **1984**, *3*, 984. (c) Farr, J. P.; Olmstead, M. M.; Balch, A. L. *Inorg. Chem.* **1983**, *22*, 1229. (d) Sutherland, B. R.; Cowie, M. *Organometallics* **1984**, *3*, 1814.
(29) Cowie, M.; Vasapollo, G.; Sutherland, B. R.; Ennett, J. P. *Inorg. Chem.* **1986**, *25*, 2648.
(30) Washington, J. S. Ph.D. Thesis, University of Alberta, 1994, Chapter 3.
(31) Jean, Y.; Lledos, A. *J. Chem. Soc., Chem. Commun.* **1998**, 1443.
(32) Schlab, P.; Mahr, N.; Wolf, J.; Werner, H. *Angew. Chem., Int. Ed. Engl.* **1994**, *33*, 97.
(33) Bender, R.; Braustein, P.; Dedieu, A.; Dusausoy, Y. *Angew. Chem., Int. Ed. Engl.* **1989**, *28*, 923.

Scheme 2

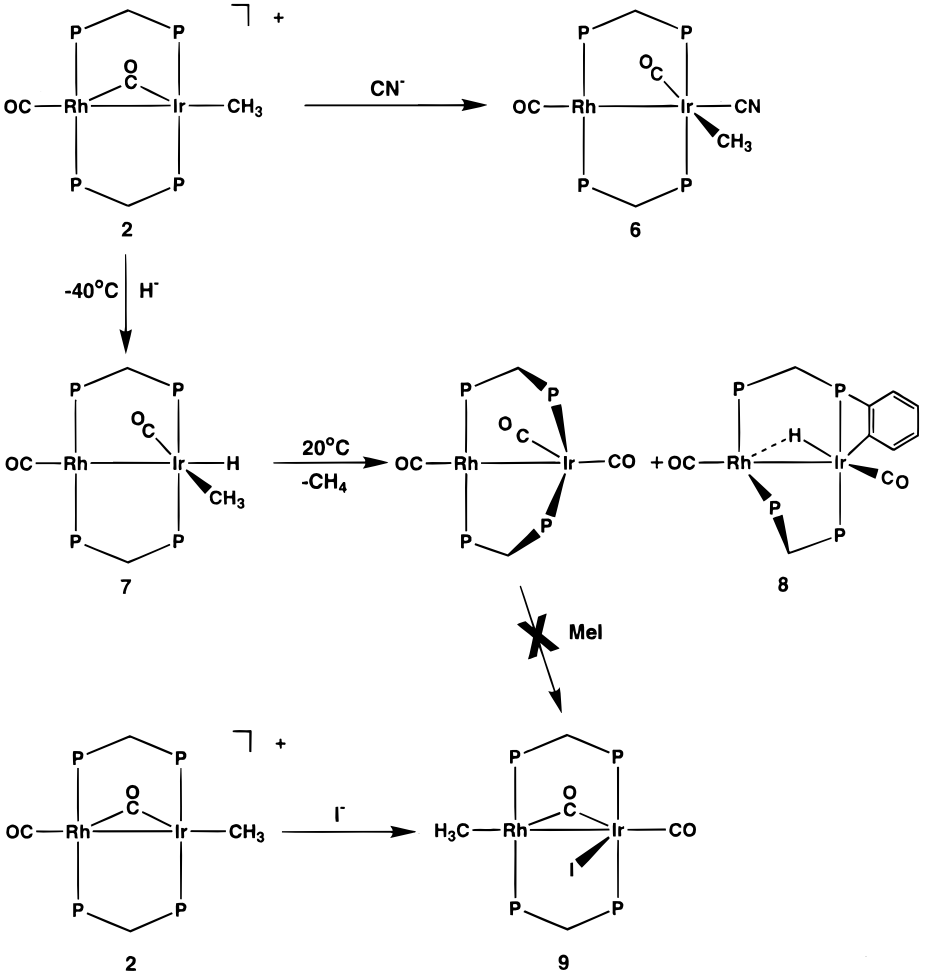

Downloaded by CARLI CONSORTIUM on June 30, 2009
Published on April 8, 1999 on http://pubs.acs.org | doi: 10.1021/om980947y

carbonyl-bridged species for **2** and a structure having a terminal carbonyl group for **5**. The carbonyl-bridged structure observed in solution for **5** seems to be the electronically favored one, in which this bridging carbonyl functions as a π acceptor for both electron-rich metals.

We had hoped that addition of another phosphine ligand to **5** might induce C−H bond cleavage, owing to the very basic metal centers that would result, or that a methyl-bridged product might result with the methyl group being forced toward Rh upon addition of the phosphine at Ir. However, the reaction of **5a** with additional PMe_3 leads to fragmentation of the "RhIr(dppm)$_2$" framework, yielding a number of unidentified decomposition products. We have previously observed dppm displacement by PMe_3 in a dirhodium complex.[34]

The reactivity of **2** with a number of anionic ligands has been investigated in order to generate neutral methyl complexes analogous to the cationic species such as **4**. With tetrabutylammonium cyanide, reaction of **2** proceeds smoothly to yield [RhIr(CH_3)(CN)(CO)$_2$(dppm)$_2$] (**6**) as shown in Scheme 2. As with the phosphines, compound **6** apparently has both the methyl group and the added CN^- anion bound to Ir. The ^{1}H NMR spectrum shows the methyl protons as a triplet at δ −0.74 with coupling to only the dppm phosphorus nuclei bound to Ir. The $^{13}C\{^1H\}$ NMR spectrum displays a triplet at 187.2 and a doublet of triplets ($^1J_{RhC} = 67$ Hz) at δ 183.8 for the Ir- and Rh-bound carbonyls, respectively. In the IR spectrum these terminal carbonyls appear at 1960 and 1932 cm^{-1}, while the cyanide stretch appears at 2084 cm^{-1}, within the normal range for terminally bound cyanide groups.[35] Although, in the absence of ^{13}C NMR data for the CN ligand, its position on Ir cannot be verified, the spectral parameters are similar to those of related neutral dialkyl complexes having this geometry,[36] for which the coordination sites of the alkyl groups can be clearly established based on $^{13}C\{^{31}P\}$ and $^1H\{^{31}P\}$ NMR experiments. The slight downfield shift of the Ir-bound carbonyl of **6** again suggests a weak semibridging interaction, as in the precursor (**2**).

Compound **2** also reacts with hydride sources such as Super-Hydride, although at room temperature several products are obtained which are difficult to characterize due to overlapping peaks. At −40 °C (and lower) several species were again observed, but the major product is identified as [RhIrH(CH_3)(CO)$_2$(dppm)$_2$] (**7**). Compound **7** shows the methyl resonance as a triplet at δ −1.02 and a hydride resonance, also a triplet, at δ −10.08 in the ^{1}H NMR spectrum; the lack of Rh coupling and selective ^{31}P-decoupling experiments establish that

(34) McKeer, I. R.; Sherlock, S. J.; Cowie, M. *J. Organomet. Chem.* **1988**, *352*, 205.

(35) Ittel, S. D.; Tolman, C. A.; English, A. D.; Jesson, J. P. *J. Am. Chem. Soc.* **1978**, *100*, 7577, and references therein.

(36) Oke, O.; Cowie, M. Unpublished results.

Downloaded by CARLI CONSORTIUM on June 30, 2009
Published on April 8, 1999 on http://pubs.acs.org | doi: 10.1021/om980947y

both ligands are bound to Ir. The $^{13}C\{^1H\}$ NMR spectrum shows one resonance as a doublet of triplets at δ 182.4 ($^1J_{RhC}$ = 83 Hz), corresponding to the rhodium-bound carbonyl and a second, broad resonance at δ 190.4 for that bound to Ir. As with compounds **2** and **6**, the downfield ^{13}C chemical shift for the Ir-bound carbonyl suggests a weak semibridging interaction.

Upon warming to ambient temperature, compound **7** transforms into two major species, along with minor unidentified products. The one product is the well-known, tricarbonyl species $[RhIr(CO)_3(dppm)_2]$,[37] which has resulted from methane loss from **7** and scavenging of a carbonyl group, presumably from the decomposition products. The other major product is $[RhIr(CO)_2(\mu\text{-}H)(\mu_2\text{-}\eta_3\text{-}(o\text{-}C_6H_4)P(Ph)CH_2PPh_2)(dppm)]$ (**8**), resulting from methane loss and subsequent orthometalation of one of the dppm phenyl groups. If a sample of **7** is allowed to warm under an atmosphere of CO, the major product obtained is the tricarbonyl complex. Compound **8** displays a complex four-resonance pattern in the $^{31}P\{^1H\}$ NMR spectrum that is characteristic of an ABCDX spin system, with the Rh-bound phosphorus nuclei at δ 6.7 and 5.6, while the two on Ir appear at δ −18.6 and −33.7. Although the Ir-bound phosphines display $^{31}P-^{31}P$ coupling of 367 Hz, characteristic of a trans alignment, no large $^{31}P-^{31}P$ coupling is observed for the other resonances, suggesting a cis arrangement at Rh. The large difference in the Ir-bound phosphines and the high-field shift of one resonance, typical of a four-membered ring,[38] suggest that orthometalation has occurred at the third-row metal. The hydride resonance in the ^1H NMR spectrum appears at δ −11.92 as a complex multiplet, and ^{31}P decoupling shows that this hydride couples weakly to Rh ($^1J_{RhH}$ = 5 Hz), consistent with a bridging arrangement in which the hydride is more strongly bound to Ir. The $^{13}C\{^1H\}$ NMR spectrum is characteristic for a species having a terminal carbonyl on each metal. Although the spectral data available are insufficient to unambiguously define the geometry, the close similarity of the spectral parameters to those of $[IrOs(H)_2(CO)_3(\mu_2\text{-}\eta_3\text{-}(o\text{-}C_6H_4)P(Ph)CH_2PPh_2)(dppm)]$[39] suggests a related geometry, and a tentative structural proposal for **8** is shown in Scheme 2.

Compound **2** also reacts with KI to give the neutral iodomethyl product $[RhIr(I)(CH_3)(CO)_2(dppm)_2]$ (**9**). However, this reaction does not proceed cleanly, and **9** is often accompanied by traces of the previously characterized diiodo species $[RhIr(I)_2(CO)_2(dppm)_2]$,[5] from which it could not be separated. Unlike compounds **6** and **7**, in which the added nucleophile and the methyl group are on Ir, compound **9** has the methyl group on Rh, as seen by the ^1H NMR spectrum in which the methyl protons, at δ −0.63, show 1.5 Hz a coupling to Rh together with coupling to the Rh-bound phosphines. In the $^{13}C\{^1H\}$ NMR spectrum one carbonyl appears at δ 212.3 with coupling of 40 Hz to Rh, consistent with a bridging group, and the other, on Ir, appears at δ 179.7. The binding of the methyl group to Rh is conclusively established by the $^{13}C\{^1H\}$ NMR spectrum of a $^{13}CH_3$-enriched sample, which shows the methyl carbon at δ 3.1 with a coupling of 22 Hz to Rh. In the IR spectrum, the one-terminal and one-bridging carbonyl formulation receives support from the carbonyl stretches at 1931 and 1761 cm^{-1}. No additional species were observed upon repeating this reaction at lower temperatures; clearly the rearrangement that brings the methyl group from Ir to Rh is facile. Compound **9** is the anticipated product (or an isomer thereof) of oxidative addition of MeI to $[RhIr(CO)_3(dppm)_2]$, followed by CO loss. But surprisingly, no reaction was observed between these reagents. This is in contrast to the facile oxidative addition of CH_3I to the diiridium analogue $[Ir_2(CO)_3(dppm)_2]$ which did give the anticipated $[Ir_2I(CH_3)(CO)_3(dppm)_2]$.[40]

Discussion

One purpose of this study was to determine the initial site of attack by substrate molecules in our heterobinuclear Rh/Ir complexes. Compound **1**, $[RhIr(CH_3)(CO)_3(dppm)_2][CF_3SO_3]$, having a 16e Rh and an 18e Ir center behaves as anticipated with attack by phosphines occurring at the unsaturated Rh center. It should be emphasized, however, that a previous study failed to identify a product of isocyanide attack at Rh, even at low temperatures.[2] So whether initial attack by other substrates at Ir can occur or whether migration of these smaller substrates from Rh to Ir is too facile to observe at the temperatures investigated is not known. Attack at the saturated metal in **1** could occur via prior transfer of a carbonyl to Rh, generating the necessary unsaturation at Ir.

Attack at the 16e/16e complex $[RhIr(CH_3)(CO)(\mu\text{-}CO)(dppm)_2][CF_3SO_3]$ (**2**) appears to occur directly at Ir in the reactions studied. Given the solid-state structure of **2**, in which the geometry at each metal is rather similar, it is difficult to envision that attack at Ir should be as kinetically favored as implied by the lack of attack at Rh observed at −80 °C. However it should be recalled that the structure in solution (**2a**) is quite different. Although both metals in **2a** have square-planar geometries, that at Rh, defined by Ir, a carbonyl, and the Rh-bound phosphorus atoms, is essentially perpendicular to the square plane at Ir, defined by the methyl, the carbonyl, and the phosphine ligands. With such a geometry, attack at Rh requires the incoming group to approach essentially perpendicular to the $RhIrP_4$ core. Such an approach should be inhibited by the four phenyl rings on either side of the $RhIrP_4$ plane and by the carbonyl and methyl groups on Ir. Attack at Ir, on the other hand, requires the ligand to approach from the end of the complex, an approach that may be more favorable, with fewer interactions with the dppm phenyl groups, and no interference from the adjacent metal.

The structures of the analogous compounds, $[RhIr(CH_3)(CO)_2(dppm)_2][CF_3SO_3]$ (**2**) and $[RhIr(CH_3)(PR_3)(CO)(dppm)_2][CF_3SO_3]$ (**5**), present an interesting dichotomy; although both solution structures differ from the structures in the solid state, both do so in opposite ways. The solid-state structure of **2** is similar to the solution structure of **5**, and vice versa. In solution, the dicarbonyl species **2** has both carbonyls terminally bound, whereas one is bridging in the solid state. For

(37) McDonald, R.; Cowie, M. *Inorg. Chem.* **1990**, *29*, 1564.
(38) (a) Garrou, P. E. *Inorg. Chem.* **1975**, *14*, 1435. (b) Garrou, P. E. *Chem. Rev.* **1981**, *81*, 229.
(39) Hilts, R. W.; Franchuk, R. A.; Cowie, M. *Organometallics* **1991**, *10*, 1297.
(40) Muritu, J.; Torkelson, J. R.; McDonald, R.; Cowie, M. Manuscript in preparation.

Downloaded by CARLI CONSORTIUM on June 30, 2009
Published on April 8, 1999 on http://pubs.acs.org | doi: 10.1021/om980947y

5, the carbonyl ligand bridges in solution and is terminal in the solid state. We view the solid-state structures as the anomalies, with intermolecular packing forces having a significant influence on the structure. For **2** the solution structure, in which each low-valent metal has one carbonyl attached, strikes us as the electronically favorable situation, and certainly this is borne out by DFT calculations on an Ir_2 analogue. Compound **5**, on the other hand, with only one carbonyl ligand, is expected to favor a bridging mode in which the ligand can function as a π acid to both electron-rich metals.

Binuclear complexes, having the metals in close proximity, are ideally suited to facile ligand migration from metal to metal. Unlike the homobinuclear Rh_2 and Ir_2 analogues, for which such migrations occur readily in the absence of added substrate, compounds **1** and **2** are static at ambient temperature. Upon addition, or in some cases removal of a ligand, rearrangements do occur, with ligand transfer from one metal to the other. One important factor inhibiting facile migration appears to be the greater metal−ligand bond strengths of Ir over Rh, favoring ligand binding to the former. This tendency is most notable for the methyl ligand, which remains on Ir in all but one example. The trend appears to be that in the cationic compounds the anionic ligand (CH_3) is bound to Ir. In the reactions of **2** with the anionic hydride and cyanide groups to yield the neutral methyl complexes $[RhIr(CH_3)X(CO)_2(dppm)_2]$ (X = H (**7**), CN (**6**)), both anionic ligands in the products are bound to Ir to yield a (formally) Rh(0)/Ir(+2) combination. The exception occurs for iodide attack in which the methyl group migrates to Rh to give the Rh(+1)/Ir(+1) compound $[RhIr(CH_3)I(CO)_2(dppm)_2]$, having one anionic group on each metal. We assume that methyl, rather than iodide, migration to Rh occurs owing to a more favorable Ir−I bond that is formed. Why the hydride and cyanide compounds do not also adopt this Rh(+1)/Ir(+1) arrangement is not clear. The structure shown for **9** in Scheme 2 is based on that of the isoelectronic diiodo analogue $[RhIr(I)_2(CO)(\mu\text{-}CO)(dppm)_2]$,[5] and this geometry is in keeping with iodide attack on **2a** at the site on Ir opposite the Rh−Ir bond (as in attack by H^- and CN^-), assuming that a merry-go-round rearrangement of ligands occurs with CH_3 movement to Rh accompanied by CO movement from Rh to the bridging site.

Our attempts to induce the terminal methyl group in **2** to adopt a bridging arrangement, through ligand addition, failed. We had thought that phosphine ligands would favor a methyl-bridged structure in order to alleviate some of the crowding at Ir. Certainly the structure of the PMe_3 adduct has severe crowding at Ir, as shown by the substantial distortions that have occurred. However, this structure maintains a strong metal−metal interaction, as shown by the alignment of the two metal centers in Figure 3. Moving the methyl group to a bridging position would substantially distort the central core, reducing metal−metal overlap. Not surprisingly, the bonding gain resulting from some type of bridging methyl arrangement would presumably be offset by the loss in metal−metal bonding.

In this study we strove to understand the roles of the different metals in the reactions of the two mixed Rh/Ir methyl complexes **1** and **2** with simple nucleophiles. The initial sites of attack (at either Rh or Ir) can be rationalized on the basis of either the site of unsaturation (Rh) in **1** or the solution structure of **2**, in which approach of substrates appears to be favored at Ir. In much of this chemistry, the rearrangements that occur appear to be driven by the stronger bonds involving the third-row metal. For the cationic species, the location of the anionic methyl group on Ir, leaving the positive charge on Rh, can be rationalized on the basis of the higher electronegativity of Ir,[41] making it more favorable for this metal to have an anionic donor ligand than the positive charge. Certainly however, a few questions remain, particularly in the neutral complexes for which structures having either Rh(0)/Ir(+2) (both anionic ligands on Ir) or Rh(+1)/Ir(+1) (one anionic ligand on each metal) are observed. It is not clear why one structure type should be favored over the other, although the tendency of the third-row congener to be in the higher oxidation state is well-known.[42]

Acknowledgment. We thank the Natural Sciences and Engineering Research Council of Canada (NSERC) and the University of Alberta for financial support of the research and NSERC for funding the P4/RA diffractometer.

Supporting Information Available: Tables of X-ray experimental details, atomic coordinates, interatomic distances and angles, anisotropic thermal parameters, and hydrogen parameters for compounds **2** and **4a**. This material is available free of charge via the Internet at http://pubs.acs.org.

OM980947Y

(41) Allred, A. L.; Rochow, E. G. *J. Inorg. Nucl. Chem.* **1958**, *5*, 264.
(42) Lee, J. D. *Concise Inorganic Chemistry*; Chapman & Hall: New York, 1996; Chapter 18.